

Hybrid Micro-Nano Robot for Cell and Cristal Manipulations

Florin Ionescu*. Kostadin Konstadinov.**
Stefan Arghir***. Dragos Arotaritei****

**Steinbeis Transfer Institute Dynamic Systems SHB, University of Applied Sciences HTWG- Konstanz, Germany (e-mail: florin.ionescu@stw.de).*

***Bulgarian Academy of Sciences-Sofia*

*** *University Politehnica Bucharest, Romania*

*****University of Medicine and Pharmacy G.T. Popa of Iasi, Romania*

Abstract: The paper presents some Computer Assisted Engineering (CAE) aspects concerning the achievement of a hybrid actuated micro-nano robot. Starting from a unitary concept Control - Design, different kinematic solutions were developed and compared, before a decision upon the structure was selected. Multiple closed loop simulations were performed via MATLAB/Simulink, Solid Dynamics and ANSYS software. The experimental results for the nano-stages/actors were run for two XY orientations with a range of 240 arcsec while and for translation in Z direction in a stroke range of 65 μ m, and system resolution of 10nm. Additional identification and reconstruction of the hysteresis curves were obtained and implemented in the model by using a Neuro-Fuzzy technique. Two hardware systems were developed for the micro and nano robot respectively. Corresponding software HMI capable also of joy-stick telemanipulation was developed.

Keywords: Robotics, micro and nano actuation, piezo drive, position and speed control, HMI, mathematical modelling, modelling and simulation, solid bodies.

1. INTRODUCTION

Robots for micro and nano manipulations are mostly used in biological and microcomputer research for cellular technology and investigation of thin films, in Atomic Force Microscopes (AFM) and Scanning Tunnelling Microscopes (STM). From a historical standpoint, the manipulators were, at first, man-operated, and then semi-automated. Thus they had a limited accuracy and productivity. For the current state of the art cellular technology, an easier insertion of probes, of electrodes or of a micro-pipette through the membrane of a single cell can only be achieved by using precise high speed steps and the appropriate actuation, a special hardware and a corresponding suitable software.

1.1 The PZT actuation

The classic actuation technologies using an AC or DC electromotor followed by a reduction drive and ball-screw drive cannot achieve the needed speed profile or the accuracy class. The use of a step-by-step electromotor offers better behaviour for low power. On the contrary, for a piezo crystal a large voltage variation corresponds to only a slight modification of physical dimensions. This so called Piezoelectric Technology (PZT) can be used to obtain a high accuracy position of under 1 μ m.

Another argument for using PZT-positioning is given by its ability to safely operate even in unfriendly strong Electro Magnetic Fields (EMF), for example in Computer

Tomography (CT) and Magnetic Resonance Imaging (MRI). Here, the manipulation system is used for applications like: bio engineering and research, for example cell positioning and penetration, tele-operated surgery, exploring micro and nano physics like the construction of nano-structures, handling a micro electrode in quality control tasks, etc.

On the one hand, position precision has to increase (<10nm) as the object size decreases, and on the other hand, the workspace has to have macroscopic dimensions (> 1cm³) to give high manoeuvrability to the system and to allow suitable handling at the border between the micro and macro worlds. For example, in transgenic applications such as injecting DNA, the insertion of a fine tube through the wall and membrane of a cell requires a fast, highly precise motion in only one the Z direction, with a displacement of 50 μ m and an angle in the XY plane in the range of milliradians.

In many situations, the total time needed to complete a positioning operation is less than 100ms, and a high average speed is needed. In more restrictive cases, a speed profile is of the essence. Thus, an average speed is not enough, but also how the speed actually evolves as a time function during the operation.

Some applications, for different numbers of degrees of freedom (DOF) and structures are presented in Burleygh (2004), LSS-2100 and LSS-2200 Cell Penetrator Systems, Ionescu et al. (2002) Micro Robots with Stewart platforms structures, or in Kleindiek Nanotechnik (2004), Klocke (1998), a Nano Motor[®] Tilting Table.

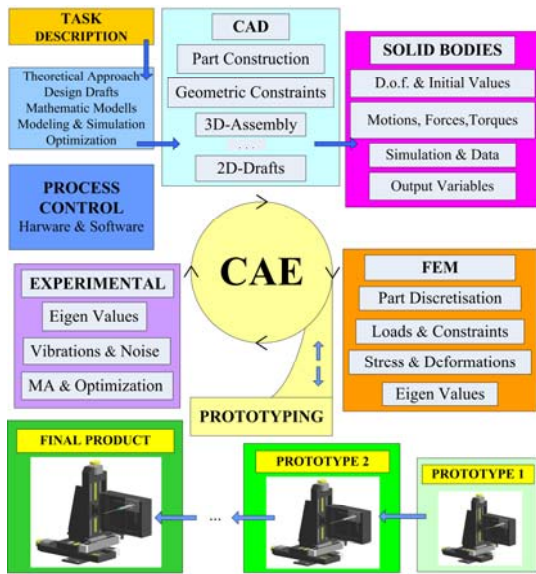


Fig. 1. Flow Chart of CAE-Development (source: F. Ionescu[©])

1.2 Applied CAE for a Micro-Nano-Robot

The four stages of the Computer Assisted Engineering (CAE) for the micro-nano robot are dedicated to obtain the highest achievable accuracy range and are depicted in 1. Starting from task formulation encompassing the main ideas, the implementation methodology, a list of performance indicators with desired values, and price margins, a first theoretical study can be started. This is based upon a (static and dynamic) nonlinear Mathematical Model (MM) given as a System of Coupled Differential Equations describing the operation of the robot, as an input-output system. For the direct dynamics one obtains the following form, after having multiplied on the right side with $[M]^{-1}$:

$$\begin{aligned} \{\ddot{q}_k\} = & -[D] \cdot [M]^{-1} \cdot \{\dot{q}_i\} - [C] \cdot [M]^{-1} \cdot \{q_i\} + \\ & + [A] \cdot [M]^{-1} \cdot \{\ddot{Q}_i\} + [B] \cdot [M]^{-1} \cdot \{Q_i\} + \\ & + [E] \cdot [M]^{-1} \cdot \{U_i\} \end{aligned} \quad (1)$$

with: $i \in [1..6n]$; $k \in [6n - 5..6n]$; $[M]$ - the inertia matrix $\{kg \text{ or } Nms^{-2}\}$; n - total number of degrees of freedom

(DOF); $[D]$ - the Damping Matrix $\{N/(m/s) \text{ or } Nm/(rad/s)\}$; $[C]$ - elasticity matrix $\{N/m \text{ or } Nm/rad\}$; $[A]$ - coefficients matrix of the first derivative of the perturbation vector $\{Q\}$; $[B]$ - coefficients matrix of the perturbation vector; $[E]$ - coefficients matrix of the input vector $\{U\}$.

Several static and dynamic nonlinearities characterize the function of each drive axis, the electric motors, amplifiers and sensors. The most common examples that occur for the designed robot are: non-diagonal matrices, nonlinear properties of slides friction and electric saturation properties of the Step Motors and Piezo Actuators. The simulation can be performed using the modelling and simulation (MS) platform. The CAD stage can now be initiated, but a direct

Solid Body supported approach could also be helpful. A first prototype can be achieved after a Finite Element Modelling (FEM). It determines displacements and critically stressed regions of parts. This information is useful for optimization. Additionally the eigenvalues and eigenforms are obtained. For research and development purposes a virtual prototyping will be obtained - which is much cheaper and with high accuracy - from the description to the simulation of virtual models. In real cases, after the first prototype is obtained, an experimental setup will help obtain the real behaviour of the static, stationary and dynamic states. In the mean time, the processor is developed: data set is defined and the appropriate control strategy is established to be implemented both in software and hardware.

1.3 Limits of Human Operator

To achieve specific performances using a human operator for micro movement process is quite difficult. And when it is facing with the nano domain, the task is quite impossible. However, this operation really depends on the operator's skills and the efficiency of this task is very low. For example, an intra cytoplasmatic sperm injection implies doing a minute operation with micrometric precision (Sittia and Hashimoto (2000), Sittia and Hashimoto (1999), Kim et al. (2001), Song et al. (2001), Friedt et al. (1999)). In this case the micro-nano manipulator is used to perform physical operations to inject genes, nucleus or embryos. Therefore, the automation of this operation using a flexible robot system drastically improves the achieved effectiveness and accuracy.

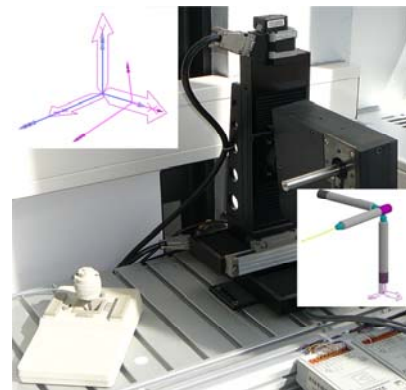


Fig. 2. Real obtained the Micro-Nano-Robot (source: F. Ionescu[©])

1.4 The Micro-Nano Robot

To overcome these limits, a nano robot with 6,5 joints was theoretically designed (Ionescu and Kostadinov (2003), Ionescu et al. (2007a), Ionescu et al. (2002), Ionescu et al. (2003a), Ionescu et al. (2004), Ionescu and Talpasanu (2006), Ionescu and Kostadinov (2007)). From the viewpoint of kinematic constraints, mechanical implementation with simulation and appropriate control are significant in practice. This present paper focuses on obtaining a CAE design of the robot as a hybrid micro-nano approach and of its appropriate control. The hybrid nature is determined in two stages, both

with direct kinematics and the individual control of each single axis. The lower level is the micro one and the higher, the nano one. The micro axes are used to position the nano stage and thus the tool in the desired workspace and with the appropriate orientation, while the nano joints are used to achieve the needed accuracy for positioning and penetration. The modelling platforms are Matlab/Simulink, Solid Dynamics Software (SDS) and ANSYS (Fig. 1).

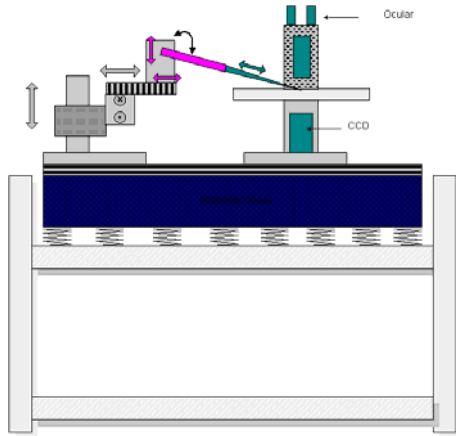


Fig. 3. Block Scheme of the 6 DOF RoTeMiNa Robot (source: F. Ionescu[©])

2. HYBRID MICRO-NANO TELEOPERATED ROBOT

2.1 Structure

High quality teleoperation and feedback critically depends on advanced mechanism designs for both master/micro and slave/nano sides. In our case they are: three stepping motor-ball-screw respectively piezo actuated nano joints slides. They provide stiff structures and linkages, actuators with small M/Force [kg/N] and J/Torque [Nms²/Nm] ratios, high reduction rates and linearity of the resolution of the position sensors. The micro and nano manipulations are achieved by using a joystick teleoperation of the system and the integration of a nano robot's with the end effector/tool into a micro positioning XYZ tables system (Fig. 3) able to places it into the referenced-working zone. The kinematic scheme to be considered is presented in Fig. 4.

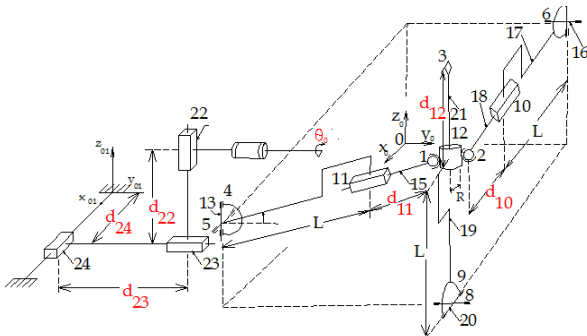


Fig. 4. Kinematic Scheme of the RoTeMiNa Robot (source: F. Ionescu[©])

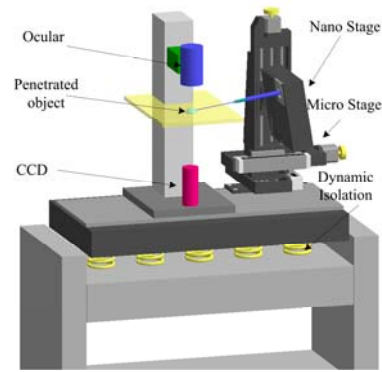


Fig. 5. The simulated nano operation stand (source: F. Ionescu[©])

2.2 Short data set

A suitable volumetric range for the considered application is $50 \times 50 \text{mm}$ for each one of the axis, thus creating a volume of $\phi 50 \times L 50 \text{mm}$. Linear axes LIMES 90 equipped with linear measuring system (resolution $0.1 \mu\text{m}$) with a repeatability of $\leq 2 \mu\text{m}$ made by OWISR (OWIS (2004)) have been chosen. Here X and Y-axis have a range of 55mm, while Z-axis, 80 mm.

2.3 Kinematics and specific joints

The linear axes are of electromechanical deformation resistant axis type (2 phase stepping motor SM240 with 200 full-steps/reverse with 2 limit switches) with zero backlash, pre-loaded recalculating ball led screw with 1 mm pitch. The nano robot was designed with 3 DOF. Two of them are rotational joints around X and Y axes in a range of 100 arcsec with actuator resolution of $1.6 \cdot 10^{-3}$ arcsec. The last joint is a translational one with a stroke of $65 \mu\text{m}$ and resolution of 1nm. The positioning sensors used here are strain gauge sensors, integrated into the actuator body with resolution of 35 nm. As a difference to the known cases, the nano robot contains, in the achieved case, one joint (a spherical type) where the end-effector is mounted directly to the link connected to the base through it. The joint here is presented in Fig. 12. The end-effector can be adjusted to the other end of the pin and has to fulfil the desired manipulation displacement/stroke (Fig. 18 and 19).

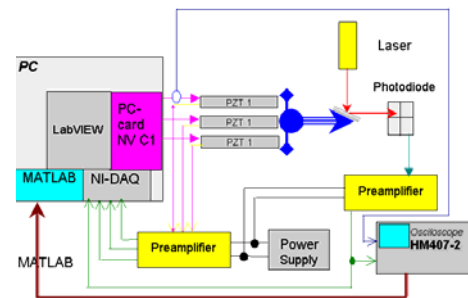


Fig. 6. Experimental set-up (source: F. Ionescu[©])

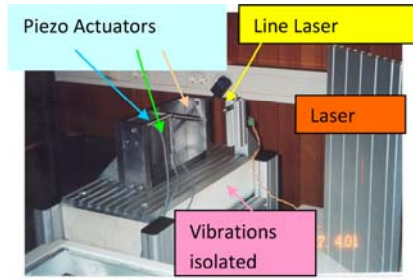


Fig. 7. Nano robot with laser unit for displacement's calibration (source: F. Ionescu[®])

3. MATHEMATICAL, SOLID BODY AND FINITE ELEMENT MODELLING AND SIMULATION

3.1 Structure Identification, Experimental Setup

The identified movement was oriented on the X, Y and Z axes of the nano-stages, using different identification methods with two different input signals: sinus and triangle.

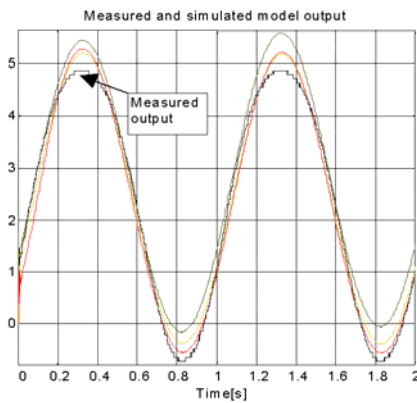


Fig. 8. Sinus displacement (source: F. Ionescu[®])

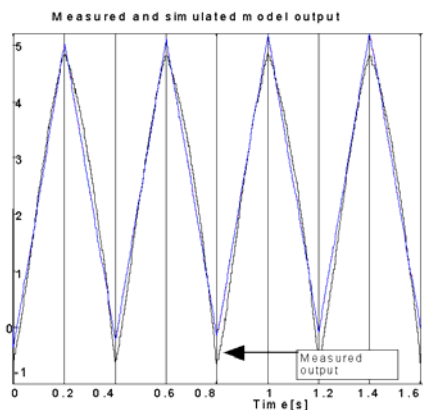


Fig. 9. Triangle displacement (source: F. Ionescu[®])

Resulting spring forces have been adjusted using the strain gauge signal in assembly process of all mechanical

components by the foreseen adjustable elements. Based on the theoretical and simulated results an experimental set-up (Fig. 6) including a nano robot prototype has been developed. (Fig. 7) The strain gauge sensors are used with a Wheatstone bridge. They operate with DC preamplifier clip module AE101 HBM[®] (Ionescu et al. (2003a)) for static and dynamic measurements (<6kHz). For data sensor acquisition, a National Instruments NIDAQ LAB PC+ board (Ionescu and Kostadinov (2007)) with the corresponding NI-DAQ 4.9 application software was used. A laser line emitter with differential diode was used to measure and calibrate the position. As a controlled power supply for the piezo actuators with capacitive loads, a PC card power supply NV C1 (Ionescu (2007)) was used.

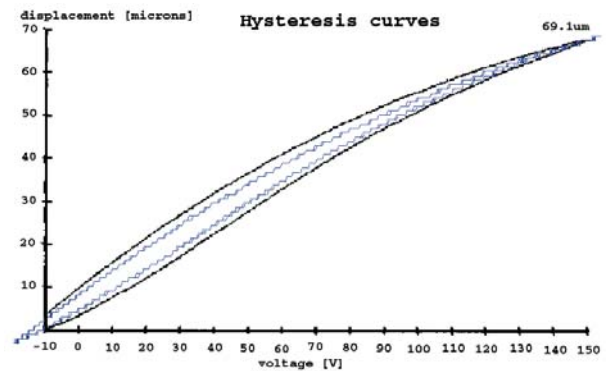


Fig. 10. Hysteresis of the Piezo Actuator PA50/14SG of X and Y (source: F. Ionescu[®])

It can drive within a nm resolution up to three axes. The experiments were done using two types of input voltage, sinus and triangle. The experimental results for orientation and translation obtained are in a range of 0-1.10 mrad and 0-65µm, with the nano robot resolution of 10nm. Results on hysteresis of the X and Y axis are presented in Fig. 6 and 7. For both cases the transfer functions has been experimentally obtained, for the same sinus and triangle inputs, using a MATLABR identification procedure, with resampling factor of 0.15, (see Fig. 8, 9) using three experimental /simulated identifications.

Via identification the transfer functions for the axis X, Y and Z were obtained. For the X axis the obtained transfer function for the sinus/triangle input signal is:

$$H_X(s) = \frac{(0.0317s^2 - 0.0287s - 0.003)}{(s^3 - 0.9997s^2)} \tag{2}$$

A comparison of theoretical and experimentally achieved identification results for the transfer functions along the X-axis obtained by Matlab/Simulink identification both for sinus and triangle input signal, the transfer function for X-axis of the nano robot here is shown below:

$$H_{Y,th}(s) = \frac{(0.0307s^2 - 0.0282s - 0.0025)}{(s^3 - 0.9997s^2)} \tag{3}$$

$$H_{Y,ex}(s) = \frac{(0.0313s^2 - 0.0273s - 0.004)}{(s^3 - 0.9991s^2)} \quad (4)$$

3.2 Mathematical Modelling and Simulation using Matlab

For these aspects we refer to the Mathematical Models 2 and 4 and in the references Ionescu and Kostadinov (2002), Ionescu et al. (2003b), Ionescu and Kostadinov (2003), Ionescu et al. (2007a), Ionescu et al. (2002), MathWorks (2005-2010). The approach opens the ways facilitates an integrated Matlab/Simulink - Control of the SD-Model, a dynamic identification and an organized optimization of the entire system: robot-control-hardware (see Fig. 13).

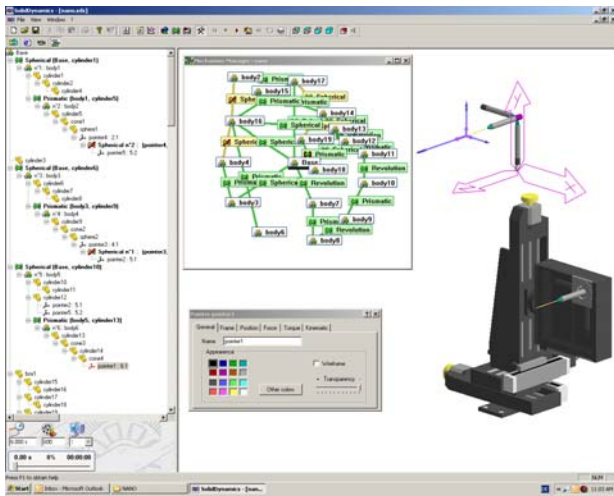


Fig. 11. SD Model the RoTeMiNa Robot (source: F. Ionescu[©])

(2006), Ionescu et al. (2003a), Ionescu et al. (2007b) and Fig. 11. The used platform was Solid Dynamics, now integrated in AIP Solid-Dynamics (2003- 2005) Motion Inventor.

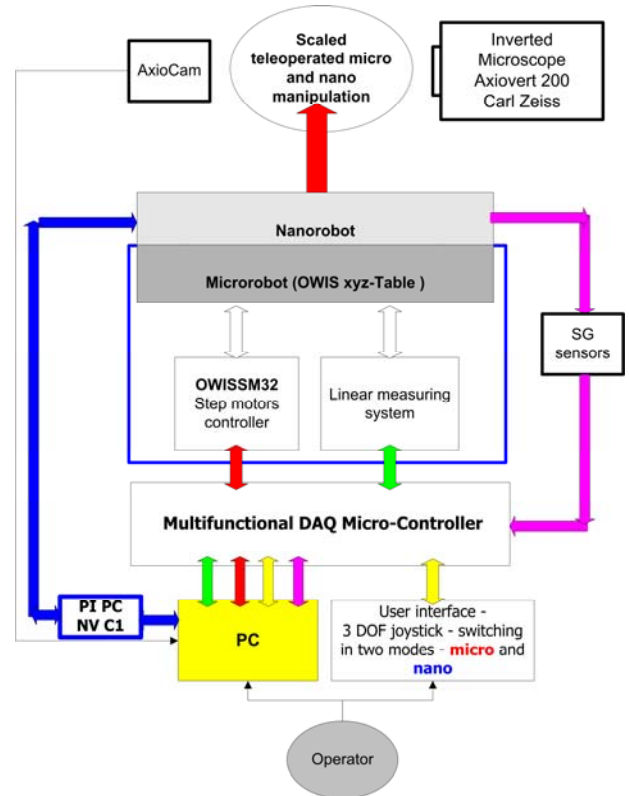


Fig. 13. Control Block-Diagram of the Micro-Nano-Robot (source: F. Ionescu[©])

3.4 Finite Element Modelling and Simulation

The FEM was applied in conjunction with the Solid Body Modelling in order to numerically validate different critical data, like: contact points, stress and deformation of some parts (Fig. 12 showing the mesh structure and the stress distribution of the holding plate). The plate is modelled with four node thin plate finite elements with 6 DOF at each node. The elastic properties of the material (spring steel with 65 % Manganese) for the plate are: E = 211 GPa and Poison ratio 0.260. For the pin (plain carbon steel with 0.45 % Carbon): E = 204 GPa and Poison ratio: 0.291. The prescribed displacement on pin bottom is applied for 30 seconds. The Coulomb friction between plate and pin is assumed.

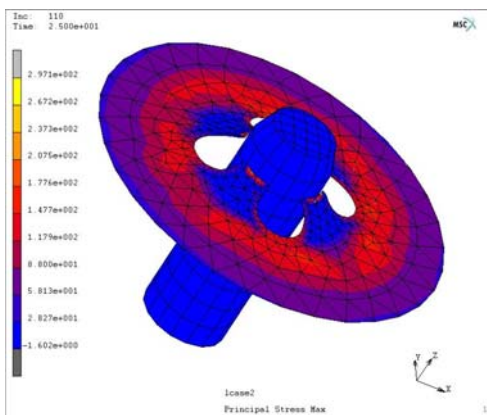


Fig. 12. Main Stress Distribution in a Plate (source: F. Ionescu[©])

3.3 Solid Bodies with SDS

The approach is facilitates visualization, feasibility estimation of movements, state-space stability study, CAD, FFT-Identification, computation of kinetic data, as: displacements, speeds and accelerations, as well as forces and torques vectors in all joints (more details in: Ionescu and Talpasanu

4. THE PROCESS CONTROL OF THE ROBOT

The control process undertakes to the process control of the entire robot, with position and speed control for 6 axes. For the process synchronization and integration of the whole micro and nano robot system, a two microprocessors Motorola MC68HC11, were used. They consist of: 1. One 12-bit Analog-Digital Converter with 8 inputs for the 3 joystick potentiometers; 2. Three 13-bit ADC's for 3 SG sensors of the piezo actuators; 3. Three inputs to read the Linear measuring system with RS-422; 4. An RS-232 or 485

interface with the PC; 5. Two digital inputs for joy-stick buttons and 6. A LCD Display 2 lines x 20 symbols (Fig. 13)

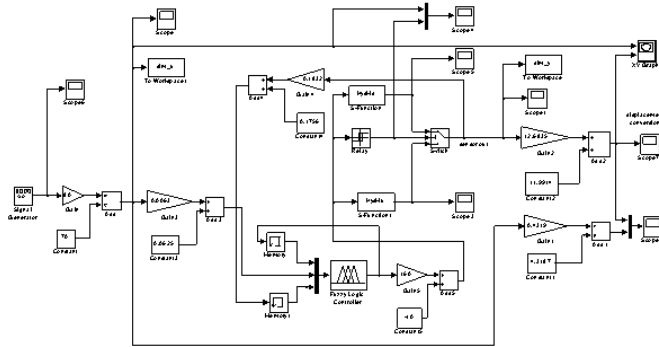


Fig. 14. The Open-loop Implementation in SIMULINK using Neuro-Fuzzy Inverse Model (source: F. Ionescu[®])

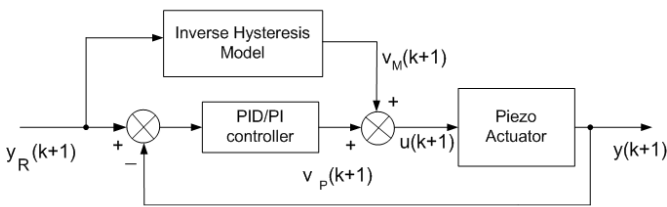


Fig. 15. The proposed structure of control system (source: F. Ionescu[®])

5. MULTIFUNCTIONAL DATA ACQUISITION MICROPROCESSOR CONTROL

5.1 Hardware

The most important tasks to be decided here is how a stable and high performing control can be obtained, in synergy with a highly variable human operator and environment dynamics, time delays in communication channel, and other effects such as hysteresis, etc. To meet this requirements the hybrid teleoperation approach is developed as a combination of a direct teleoperation and a task oriented teleoperated manipulation (Fig. 13) via PC keyboard and a master joystick and visual feedback via Carl Zeiss Microscope Axiovert 200 Zeis (2005b) equipped with AxioCam HRm with basic resolution of the sensor 1300x1030 pixels Zeis (2005a) and AxioVision software. A joystick MACH-IV for the manual command 6 DOF, with start and stop button for automatic execution of cell penetration and a switch mode button was implemented. The last one is used to switch the nano stage robot and the macro positioning guidance of the micro robot structure as well, in order to perform the desired nano manipulation (Fig. 2 and 19).

5.2 Control

A control diagram was proposed in order to compensate the hysteresis of piezo actuators included in micro/nano robot

(Fig. 14). The schema uses a Neuro-Fuzzy inverse model with PID/PI error mapping compensator. We adopted an

originally mixed algorithm in order to tune the PID/PID parameters using GEATbx toolbox. The simulation results proved that our method is very effective, with a very good linearization of the hysteresis curve even in the case of a very sharp upper a lower corner of hysteresis. The Mean Square Error (MSE) was below 0.005 in all the tested cases. The control schema is based on inverse Neuro-fuzzy model in a feed-forward connection. The piezo-actuator is modelled by modified mathematical model in order to be simulated and to be tested in a mixed analogue-discrete schema. The mapping errors due to dynamic fuzzy model are compensated by PID/PI controllers (Fig. 15). The PID/PI parameters are found using genetic algorithms applied to global optimization problem with two objectives. The Pareto front that describes the optimal solutions is found using rank-based selection for local points that describe the Pareto front (Fig. 16). The proposed method improved noticeably the linearization of the hysteresis and the performance of the piezo-actuator.

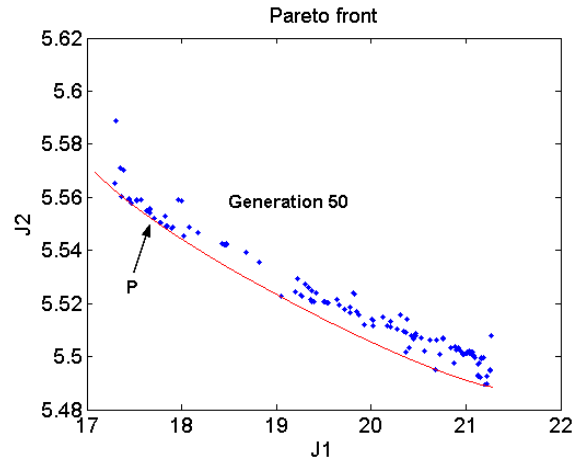


Fig. 16. The Pareto Front (PF) after 50 generations (source: F. Ionescu[®])

The point P indicates the selected individual for PID tuning parameters (TP, TI, and TD). For the control of micro and nano robots two approaches, namely teleoperation approach or automatic manipulation are utilized. The direct teleoperation approach can realize tasks requiring high level intelligence and flexibility. It is slow, not so precise, not exactly repeatable and affected by many complex and challenging scaling problems. However, the task-oriented approach avoided those problems by executing only the given task in closed loop autonomous control (Sitti et al. (1998)).

5.3 Scaling

It is one of the most important factors for successful performance of the teleoperated micro and nano manipulation since there is a large difference in the scale between the human operator (master joystick) and slave/nano robot. There are basically two approaches are basically used: linear and nonlinear scaling.

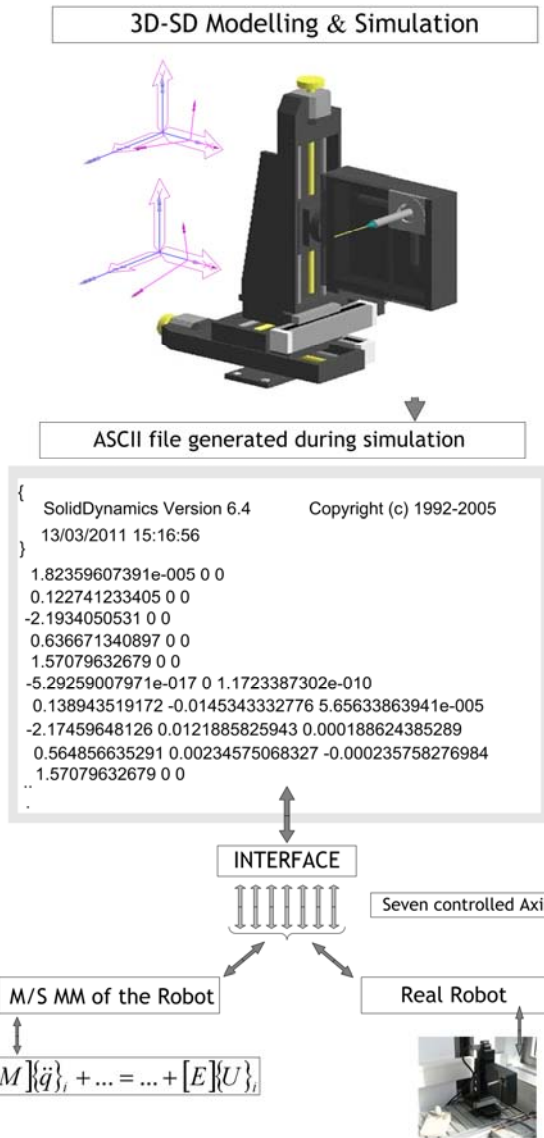


Fig. 17. Control interface in SD and MS (source: F. Ionescu[©])

Linear scaling In this case a single corresponding constant is used between the nano/micro robot positions and the macro joystick angular positions: $\phi_{i,j} : x_{R,i} = \alpha_{s,i} \cdot \phi_{j,i}$. The human operator has no perception about the robot end-effector dynamics and the space size in which it manipulates. Hence, in the case of cell micro and nano manipulations a haptic interface has to provide the operator with the feeling that he knows the dynamics of the objects to be manipulated.

Nonlinear scaling It is achieved by introducing a virtual mechanical appropriate impedance $Z_{s,i}$. The robot dynamics can be assigned to virtual couple mechanical impedance Z , appropriately to the operator to manipulate in the micro/nano world, as follows: the macro joystick angular positions define the force F_i by which the robot axes will be driven, by: $F_i = z_{s,i} \cdot \phi_{j,i}$. Thus the teleoperation controller can realize proper coupling between the macro and nano world.

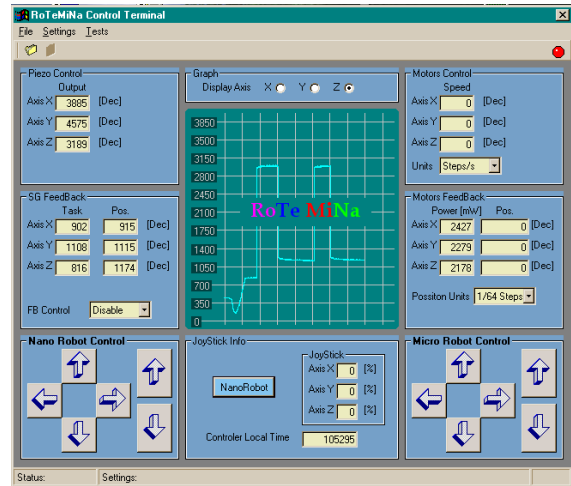


Fig. 18. Control menu of the two robots stages (source: F. Ionescu[©])

5.4 Controlling and validating the model

The most important tasks are to find out how stable and high performance in the real conditions the control can be obtained: the human operator, the dynamics environment, time delays in communication channel, hysteresis, etc. For an obtained robotic model, the SDS simulation environment can send the position of all the joints to the real robot. By using an ASCII file, the positions of all the joints relative to time can be imposed on the real counterpart so as to compare both of them simultaneously (Fig. 17). By observing the differences between the real and the modelled robot one can improve the real prototype.



Fig. 19. Experimental set-up for cell penetration (source: F. Ionescu[©])

5.5 Experimental Setup

A visual feedback can be obtained by using a Carl Zeiss Microscope Axiovert200 Zeiss (2005b) equipped with

AxioCam HRm with basic resolution of the sensor 1300x1030 pixels Zeiss (2005a) and AxioVision software (Fig. 19). The Joystick MACH-IV has 3 DOF, a start/stop button for automatic execution of cell penetration and a switch mode button. The last one is used to switch either the macro positioning guidance of the regional robot structure in micro mode or to perform desired nano manipulations in nano mode.

6. CONCLUDING REMARKS

The RoTeMiNa robot with 6.5 DOF was, including the HMI, designed, mathematically and 3D-modeled, simulated, optimized, constructed and experimentally tested. For this purpose, a circuit board was also developed to support and control the hardware, software, control menu, joystick, etc. The identification of the nano structure was executed using MATLAB[®] libraries, and compared with the experimental results for the X, Y and Z axes for different identification methods and two different types of the input signal.

ACKNOWLEDGEMENTS

The project Micro-Nano-Robot RoTeMiNa, from which the paper presents a short resume, was funded by Steinbeis Foundation Stuttgart, DFG and DAAD Bonn, University of Applied Sciences Konstanz, Germany as well as by Bulgarian Academy of Sciences. Towards all these organizations the authors are expressing their warm gratitude.

REFERENCES

- Burleigh (2004). Burleigh Instruments inc., USA. <http://www.burleigh.com>.
- Friedt, J.M., Hoummady, M., and Cervelle, J. (1999). Remote controlled tele-nanomanipulation. In *Proceedings of the IEEE/ASME International Conference on Advanced Intelligent Mechatronics*, 9-12. Atlanta, USA.
- Ionescu, F. (2007). Complex modelling in mechatronics. In *Proceedings of CSCS 16th International Conference on Control Systems and Computer Sciences and 3rd International Symposium on Interdisciplinary Approaches in Fractal Analysis IAFA*, volume 3, 2-16. ARTECH Edition, Bucharest, Romania.
- Ionescu, F. and Kostadinov, K. (2002). Piezo actuated robot for micro and nano manipulations. *ARA-Journal*, 2000-2002(25-26), 98-106.
- Ionescu, F. and Kostadinov, K. (2003). Robot for micro and nano manipulations. In *Proceedings of National Colloquium of Teaching and Scientific Research*, 9-17. Credis Edition, Bucharest, Romania.
- Ionescu, F. and Kostadinov, K. (2007). Cell micro and nano manipulations with a hybrid robot. In T.C. Yih and I. Talpasanu (eds.), *Micro and Nano Manipulations for Biomedical Applications*, 215-252. Artech House, Boston, USA, 1st edition.
- Ionescu, F., Kostadinov, K., and Hradynarski, R. (2004). Operation and control a 6,5dof micro and nano robot for cell manipulations. In *Proceedings of the IEEE MechRob 2004 Conference*, volume 3, 931-935. Aachen.
- Ionescu, F., Kostadinov, K., Hradynarski, R., and Vuchkov, . (2003a). Teleoperated control for robot with 6 dof for micro and nano manipulation. In *Intelligente technische Systeme und Prozesse*, volume 3, 127-132. Logos Verlag, Magdeburg.
- Ionescu, F., Kostadinov, K., Hristov, K., Hradynarski, R., and Vuchkov, I. (2002). Operation and control of piezo actuated robot for cell micromanipulations. In *47th International Wissenschaft Colloquium*, volume 3, 135-143. ARTECH Edition, Ilmenau, Romania.
- Ionescu, F., Talpasanu, I., Arotaritei, D., Hradynarski, R., and Kostadinov, K. (2007a). Intelligent control of piezo actuated robot using and approximated hysteresis model. In *Proceedings of the 16th Intern Conference on Control Systems and Computer Science, CSCS*, volume 3, 220-231. ARTECH Edition, Bucharest, Romania.
- Ionescu, F., Talpasanu, I., Kostadinov, K., Hradynarski, R., and Arotaritei, D. (2007b). Closed chain mechanism of micro and nano robot for cell manipulations. In *Proceedings of the IASTED International Conference RA07*, 340-345. Würzburg, Germany.
- Ionescu, F. and Talpasanu, I. (2006). Teleoperation hybrid robot for cell micro and nano manipulations. In *Proceedings of the NanoBio 2006 IEEE/ASME Conference on Frontiers in Biomedical Devices*. Irvine, USA.
- Ionescu, F., Kostadinov, K., Hradynarski, R., and Vuchkov, I. (2003b). Operation and control of 6 d.o.f. robot for cell manipulations. In *Proceedings of the Annual World Conference of ARA`28*, 779-782. Târgu-Jiu, Romania.
- Kim, D.H., Kim, K., Kim, K.Y., and Cha, S.M. (2001). Dexterous teleoperation for micro parts handling based on haptic/visual interface. In *Proceedings of the IEEE Intern Symp on Micromechatronics and Human Science*, 211-217. Nagoya, Japan.
- Kleindiek Nanotechnik, R.G. (2004). <http://www.nanotechnik.com/mm2.html>.
- Klocke, D.V. (1998). Motion from the nanoscale world. CD-ROM.
- MathWorks (2005-2010). MATLAB/Simulink.
- OWIS (2004). Owis. <http://www.owis-staufen.de>.
- Sitti, M., Hoummady, M., and Hashimoto, H. (1998). Trends on mechatronics for micro/nano telemanipulation: Survey and requirements. In *IFAC Informational Control in Manufacturing*, 235-240.
- Sittia, M. and Hashimoto, H. (1999). Teleoperated nano scale object manipulation. *Recent Advances on Mechatronics*, 322-335.
- Sittia, M. and Hashimoto, H. (2000). Two-dimensional fine particle positioning under optical microscope using a piezo resistive cantilever as a manipulator. *Micromechanics*, 1(1), 25-48.
- Solid-Dynamics (2003-2005). Solid Dynamics Software.
- Song, E.H., Kim, D.H., Kim, K., and Lee, J. (2001). Intelligent user interface for teleoperated micro-assembly. In *Proceedings of the International Conference on Control, Automation and Systems*, 784-788. Nagoya, Japan.
- Zeiss (2005a). AxioCam. <http://www.zeiss.de/axiocam>.
- Zeiss (2005b). Micro. <http://www.zeiss.de/micro>.